MULTI-BAND PHOTOMETRIC OBSERVATIONS OF GEO SATELLITES: PRELIMINARY RESULTS

A. Di Cecco(1,3), F. De Luise(1), C. Marzo(2), C. Portelli(3), M. M. Castronuovo(3) and G. Valentini(1)

(1)*National Institute for Astrophysics (INAF), Observatory of Teramo, via M. Maggini snc, TE 64100, E-mail: {dicecco,deluise,valentini}@oa-teramo.inaf.it*
(2)*Italian Space Agency (ASI), Center for Space Geodesy, c.da Terlecchia, Matera 00175 I, E-mail: cosimo.marzo@asi.it*
(3)*Italian Space Agency (ASI), via del Politecnico snc, Rome 00133 I, E-mail: {claudio.portelli,marco.castronuovo}@asi.it*

ABSTRACT

The Observatory of Teramo has been recently involved in the study of the space debris in the framework of the agreement between the National Institute for Astrophysics (INAF) and the Italian Space Agency (ASI). The Observatory hosts the Teramo Normale Telescope (TNT), a 72 cm optical telescope equipped with a Charge-Coupled-Device (CCD) camera of 1024x1024 pixels and a Field-Of-View (FoV) of ~5x5 square arcminutes. An alternative CCD camera of 3296x2472 pixels, with a FoV of ~11x15 square arcminutes, is also available. Both CCDs have a resolution scale of 0.27"/pixel. A filter-wheel mounting Johnson optical filters (B, V, I, R) is also usable for multi-band photometric observations.

In order to investigate the attitude and the surface materials of the space debris, we have started an observational campaign with the TNT telescope focused on the GEO objects.

In this paper, we present the preliminary results obtained for the EXPRESS AM7 satellite. In particular, we acquired 79 multi-band scientific images, in two different nights, by using different filters and exposure times. We pre-reduced the images by correcting them for the instrumental effects, by using bias, dark and flat-field frames. We provided an absolute aperture photometry and we reconstructed the lightcurves for each filter in order to analyze the brightness distribution across time.

The preliminary results seem to suggest that in the redder R and I bands there are larger brightness variations, with the occurrence of significant minima, likely related to the intrinsic features of the satellite. However, before being able to confirm this slight evidence more observations and analysis are required.

Key words: Multi-band photometry; space debris; optical data; lightcurves.

1. INTRODUCTION

Space debris population is a big problem for many space activities. Theoretical simulations estimate more than one billion of pieces smaller than 1 cm, a number of ~670,000 pieces in the range between 1-10 cm, and ~29,000 pieces of larger size. In order to maintain space safety and estimate the risk related to space debris, it is necessary to reconstruct their orbits as well as to characterize their physical properties.

Space debris population has been mainly investigated by using optical and radar instruments. In particular, the ground-based optical telescopes allow us to observe up to the farthest GEO region ($\approx$ 36,000 km). Within the optical observations, the multi-band photometry has demonstrated to provide essential constraints for the space objects characterization.

In order to investigate the composition of the surface materials of space debris, the observed (BVRI) Johnson photometric color-indexes were compared with the laboratory measurements of the common materials used in the spacecraft manufacturing [7, 12, 4]. Interesting observational results were also provided by using both photometric and spectroscopic images [2, 9]. Moreover, the study of the photometric brightness distribution across time provides essential constraints on the spatial attitude and structure of space objects. In particular, by reconstructing optical lightcurves, the rotational period and tumbling have been investigated [3, 10, 11]. The tumbling motion of GEO satellites have been also recently studied by providing infrared lightcurves in JHK bands [14].

Several theoretical efforts show that lightcurves are good indicators of the main components of space objects. For instance, the spacecrafts with two-wing solar panels present double peaks in brightness distribution, while one-wing structures have one peak [5]. Theory also suggests that the lightcurves investigation provides information on the surface materials through their

Proc. 7th European Conference on Space Debris, Darmstadt, Germany, 18–21 April 2017, published by the ESA Space Debris Office
Ed. T. Flohrer & F. Schmitz, (http://spacedebris2017.sdo.esoc.esa.int, June 2017)

reflective properties [8]. The theoretical framework takes into account both intrinsic features and external lighting conditions, such as the albedo coefficient, the surface materials and the Sun phase angle [5, 13].

2. CURRENT FRAMEWORK

In order to test existing national facilities for space debris observations ASI has signed a three-years cooperation agreement with INAF, from 2016 to 2018. In particular, several optical and radio telescopes are currently involved in observational campaigns at different latitudes (Lat 38°–45° N) and longitudes (Long 11°–14° E). For what concerns optical observations, small optical telescopes of $\lesssim$1.5 m diameter are used.

In the following sections, we present the scientific analysis of multi-band photometric data of GEO satellites, acquired with the optical telescope of the INAF Observatory of Teramo (OATe).

Unfortunately this Observatory is located at about 30-40 km from the epicenter of the earthquake swarm that hit Central Italy from August 2016 to January 2017, with magnitude $\approx 5 - 5.5$. This inconvenience has partially limited the telescope observational time during the first year of the agreement.

2.1. The Observatory

INAF-OATe is located at 398 m o.s.l, in the homonymous city of Teramo, in the Abruzzo Region. Its latitude and longitude are respectively 13.73° E and 42.65° N.

At the present time, the number of people working at the OATe is about thirty, including researchers, engineers, technicians and administrative staff. The main goals of the scientific research carried out in the OATe are following:

- Stellar evolution and population synthesis
- Galaxies evolution
- Type Ia Supernovae progenitors
- Solar System exploration (Mars)

In these fields, the INAF-OATe researchers have developed strong skills in the theoretical simulations and in the analysis of data from the visible to the far infrared wavelengths, both in photometry and spectroscopy, as proven by the high number of papers produced each year, as well as by the numerous collaborations with several Institutes and Universities worldwide.

Moreover, many technical projects have been developed at OATe, and many contributions have been provided to several projects, such as SKA, MAORI, AMICA and active optics cameras.

Table 1. CCD details

Format	3296x2472 pixels
Scale	0.27 arcsec/pixel
FoV	15x11 arcminutes
Dark current	0.05 e$^-$/pixel
Gain	1.35 e$^-$/ADU
Read Out Noise	7 e$^-$
Dynamics	16 bit
Filters	B,V,R,I

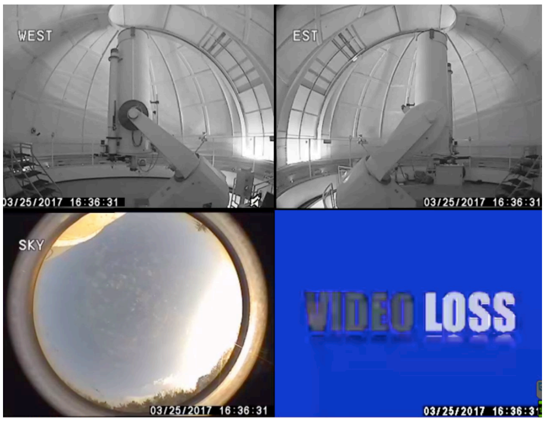

Figure 1. The four screens visible from the remote videoserver. Top panels: the TNT left and right sides, as seen by the two cameras inside the dome. Bottom panels: the sky as seen from the external camera on the left , and the finderscope camera (switched off at the day time) on the right.

2.2. The instruments

In order to observe GEO satellites we have used the TNT (Teramo-Normale-Telescope), a small-class optical telescope mounting a mirror of 72 centimetres.

The TNT has an optical layout of a typical Ritchey-Chretien design, with a focal ratio of f/14. At the time of the acquisitions described below, a CCD of 3296x2472 pixels, with a resolution of 0.27″/pixel and a total FoV of ≈11x15 square arcminutes was located in the telescope focal plane.

The TNT telescope is also equipped with a rotating filter-wheel mounting the four BVRI filters of the Johnson-Cousins photometric system, available for the wavelength range between ≈ 0.44 and ≈ 0.87 μm [1]. This last feature allows us to provide a multi-band photometry.

The TNT and CCD camera technical details are listed in Tab.1.

The telescope and the dome are completely operable by remote control, available through the authentication to a security system. In particular, by using the re-

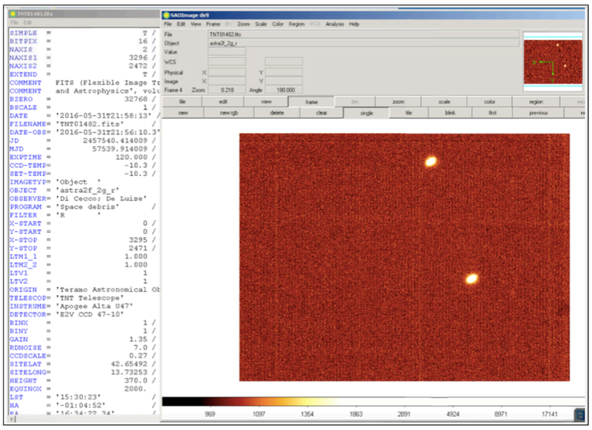

Figure 2. An image acquired by the TNT of the two GEO satellites ASTRA 2G and ASTRA 2F (in the R band).

mote controls we are able to manage all the power supplies, telescope pointing and tracking system, CCD work-temperature setting and acquisition modes. Moreover the dome is completely automatized and synchronized to the telescope movements.

A local weather station is also present and connected to the web to monitor the weather conditions. It is possible to view simultaneously up to four screens using a videoserver from any remote location (see Fig.1). Usually, two screens are for the two cameras pointed inside the dome, one screen is for the external weather camera and the last is for the images of the finderscope 1.

Generally, the main difficulties in using small FoV for GEO observations are related to the high accuracy knowledge of the object coordinates, usually ∼1–2 arcminutes. If the accuracy is high enough, however, multiple satellites belonging to same constellation can also be caught together in the same image. For instance, Fig.2 shows the two GEO satellites ASTRA 2G and ASTRA 2F observed simultaneously within the same TNT frame. Moreover, the signal-to-noise ratio between the photon count at the source peak and the background mean level is significantly high (S/N∼10).

3. OBSERVED TARGET

The observed scientific target is EXPRESS AM7, a GEO communications satellite operated by the Russian Satellite Communications Company (RSCC, see Fig.3). EXPRESS AM7 is also known with the COSPAR ID 2015-012A and NORAD catalogue n. 40505.

The satellite was manufactured by Airbus DS (formerly EADS Astrium) and launched on 18th March 2015 by a Proton-M rocket, from the Baikonur spaceport of Kazakhstan. The total mass at launch was of the order of 5,700 kg, while the payload mass is ∼ 1,500 kg. The mission lifetime is planned to be 15 years.

Figure 3. An image of EXPRESS AM7 as taken by the website www.aerospace-technology.com on courtesy of RSCC.

The satellite hosts 62 active transponders 24 in C-band, 36 in Ku-band and 2 in L-band. Three-section solar panels provide an electric power of ∼ 18 kW.

The longitude of the EXPRESS AM7 orbit is 40° E and the inclination is approximately 0.02°. Its orbit shows no sensible drift with respect to its nominal equatorial position. This feature made EXPRESS AM7 a good choice for our first investigation on the GEO satellites.

4. OBSERVATIONAL DATA

The observing runs were conducted in the nights of 28th May and 29th July 2016. In the following we refer to these nights as to the *first* and the *second* nights respectively.

During the two nights a total of 79 scientific images[1] of EXPRESS AM7 were acquired. In detail, 30 images were provided during the first night by using the V, R and I filters: 10 images for each filter, with exposure time of 60 s each. The other 49 images were acquired in the second night by using four bands B, V, R and I. In the last case, different exposure times were used. The details of the entire dataset are listed in Tab2.

The exposure times were chosen after several observational tests considering as a target a S/N of at least 8–10, for the ratio between the photon counting at the maximum peak of the object and the surrounding sky background.

For the acquisition of the EXPRESS AM7 images, the TNT telescope was operated at fixed position, in non-sidereal tracking mode.

In order to calibrate the scientific images for the instrumental response, several calibrating frames were also ac-

[1] The TNT data are in the common FITS (Flexible Image Transport System) open standard.

Table 2. Scientific data. In the columns are listed the used filters, the number of images per filter, the exposure time, the start and end observational times.

First night – 28^{th} May				
Filter	N. images	Exp. Time [s]	Start time [hh:mm:ss]	End time [hh:mm:ss]
B	–	–	–	–
V	10	60	21:29:52	21:40:15
R	10	60	21:41:24	21:52:48
I	10	60	21:52:57	22:03:20
Second night – 29^{th} July				
Filter	N. images	Exp. Time [s]	Start time [hh:mm:ss]	End time [hh:mm:ss]
B	7	550	21:05:53	22:03:00
V	21	180	20:54:36	23:04:15
R	13	180	23:04:38	23:48:55
I	8	300	23:54:30	00:34:27

quired. In particular, for each night, we acquired 5 dark current and 5 bias frames, as well as we provided 5 images for the flat–field in each filter by using dome lamp.

4.1. Reduction strategy

In order to analyse the acquired data, first of all, we pre-reduced the raw scientific images by applying instrumental calibration procedures. We calculated the median image of the dark and bias, and we subtracted them from the flat–field and the scientific images. We calculated the median flat–field image for each filter and we normalized the obtained median frame to its mean pixels value. We divided, then, each scientific image for the normalized median flat–fields, using the following formula:

$$\text{Reduced Image} = \frac{(Raw\ image - Bias - Dark)}{<(Flatfield - Bias - Dark)>}$$

To reduce the images we used the tasks of IRAF (Image Reduction and Analysis Facility), a free data analysis software released by the NOAO (National Optical Astronomy Observatory[2]). In particular, we used the *imcombine*, *imarith* and *imstat* tasks, respectively to obtain the median images, to subtract or divide frames, and to have the mean statistical value.

During data reduction we analysed the images by visual inspection, in order to overcome overlapping field stars that may compromise the magnitudes measurement.

To calculate the magnitudes, we used the aperture photometry technique. For this purpose, we integrated the pixel values within a circle centred around the source and then we subtracted the background level by using an external annulus. In particular, we used radii of ≈ 20 and 50 pixels for the inner and the outermost annular regions. The aperture photometry was provided by using the IRAF task *phot*.

[2] https://www.noao.edu

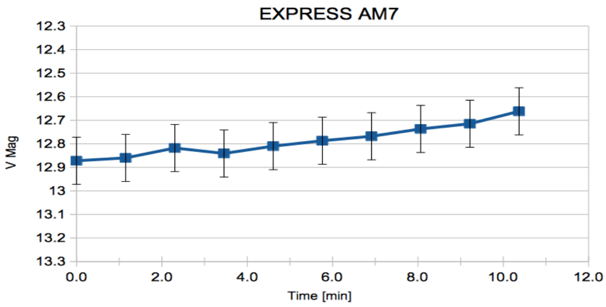

Figure 4. Lightcurve of the V band for the first night.

Absolute calibration to the standard system has been provided by using standard fields [6]. However, owing to instrumental problems related to technical operations during the observations, standard calibration fluxes have large photometric errors. Taking into account this issue, we estimated an upper limit of $0.1 - 0.4$ mag for the accuracy of the magnitudes.

5. DATA ANALYSIS

Hereafter we present the analysis of the observational lightcurves of EXPRESS AM7, by discussing briefly the results obtained for each night and each filter.

For the first night, we obtained three (VRI) lightcurves, each covering a time interval of 10 minutes.

The V magnitudes are shown in Fig.4. The distribution suggests that in the V band the flux increases continuously, with a difference between the maximum and minimum magnitudes of Δ_{min}^{max} ≈0.21 mag. The mean magnitudes value is ≈12.78 mag.

The magnitudes registered in the R images, acquired soon after the V images, are shown in Fig.5. In this case, the brightness changes rapidly in 10 minutes, approaching a minimum value of 16.53 mag and a maximum value of 15.79 mag (Δ_{min}^{max} ≈0.74 mag), with a mean value of ≈16.16 mag.

A fast variability is also shown by the I magnitudes, presented in Fig.6. The lower magnitude limit for the I band is ≈16.45 mag, while the maximum value is ≈17.00 mag, with a difference of Δ_{min}^{max} ≈0.55 mag.

By using the second night's data, we obtained four lightcurves in the B, V, R and I filters, covering different time intervals.

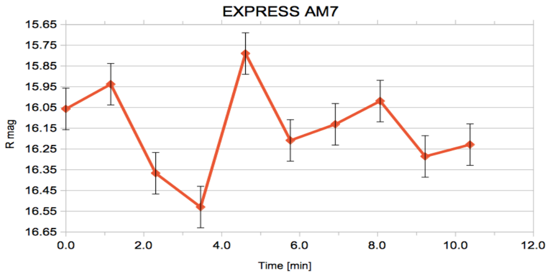

Figure 5. Lightcurve of the R band for the first night.

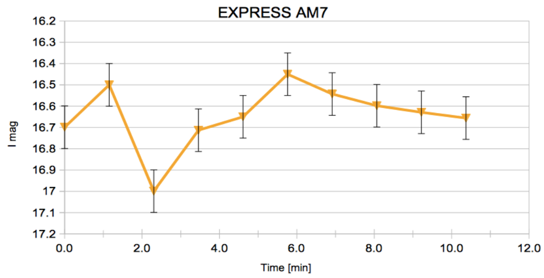

Figure 6. Lightcurve of the I band for the first night.

The V lightcurve extends for ≈2.30 hours. The first 6 images of the V filter were acquired alternating the V with the B bands (see following).

The V magnitudes distribution has a mean value of ≈18.30 mag, with a maximum of ≈18.80 and a minimum of ≈17.80 mag (Fig.7). Note that when considering longer time range with respect to the first night, the V magnitude shows higher difference variations (Δ_{min}^{max} ≈1.00 mag) .

The R magnitudes distribution covers a time range of approximately 45 minutes. The mean value is ≈18.60 mag, if excluding the occurrence of a significant brightness minimum at ≈19.50 mag (exceeding 3σ from the average). In this case the difference between the maximum and minimum magnitudes is Δ_{min}^{max} ≈1.20 mag. The R lightcurve is shown in Fig.8.

The I data cover a time range of ≈ 40 minutes. In this case, the mean value of the brightness distribution shows a slow decrease from ≈19.00 mag to ≈ 20.00 mag (Δ_{min}^{max} ≈1.0 mag). The lightcurve is plotted in Fig.9.

During the second night, as mentioned before, the B filter was also used. The B images were taken in a time interval of 1 hour and the magnitude distribution in shown in Fig.10. The brightness value increases for the initial 40 minutes, from ≈19.55 mag up to ≈19.10 mag, then a minimum of ≈19.8 mag appears (Δ_{min}^{max} ≈0.70 mag). This seems to be a plateau (two points) before the minimum, but it cannot be considered a firm conclusion owing to low statistics.

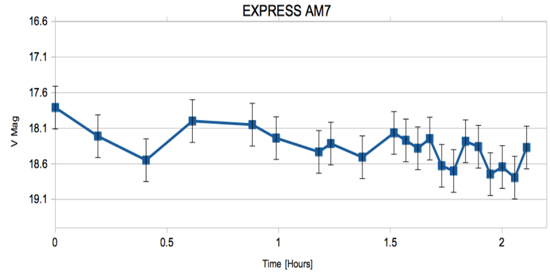

Figure 7. Lightcurve of the V band for the second night.

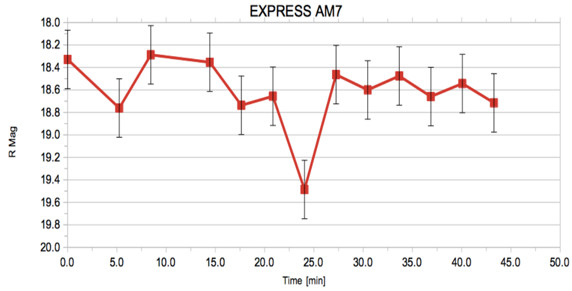

Figure 8. Lightcurve of the R band for the second night.

In order to investigate the occurrence of a correlation between the V and B filters, these two bands were alternated during the first hour of observations. By comparing the V and B lightcurves, the values of the brightness are in the B filter are always lower than in the V band. Moreover, no correlation is shown. These results are presented in Fig.11, where lightcurves are plotted together. In the same figure, the magnitudes of the other bands are also plotted, by using the same reference time. Fig.11 shows that in the optical filters the magnitude values are in the range 18-20 mag. Moreover, the distribution plotted in Fig.11 seems to suggest a slow decrease of the mean magnitude value, when moving from the shorter to longer wavelengths (if excluding the B filter). However, before being able to confirm this behaviour, more observations are required, and the Sun angle phase has to be considered.

6. CONCLUSIONS

This investigation presents the preliminary results obtained by using the TNT telescope for GEO satellites observations. In particular, we observed the EXPRESS AM7 satellite in two different nights, by collecting 79 scientific images in the BVRI Johnson bands. We

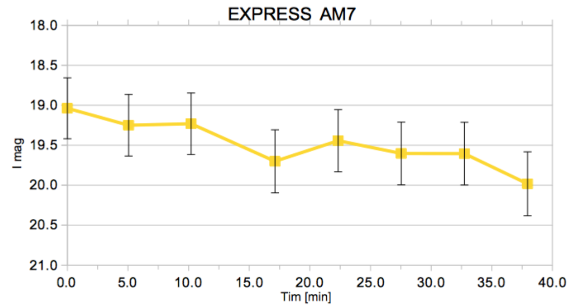

Figure 9. Lightcurve of the I band for the second night.

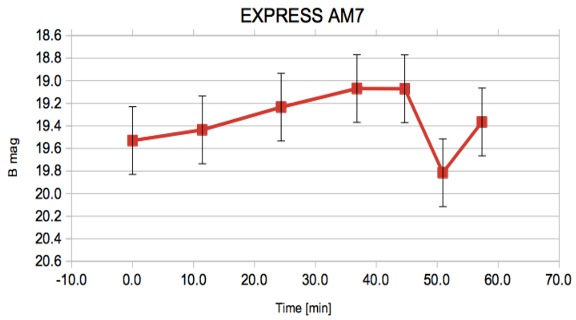

Figure 10. Lightcurve of the B band for the second night.

reduced the data by providing an absolute aperture photometry. In order to investigate the magnitudes distribution of EXPRESS AM7, we reconstructed the photometrical lightcurves. During the same night the lightcurves varied within the range of ≈1–1.2 mag. However, when comparing different nights, a different behaviour was observed. In particular, the average value of the magnitudes for each filter changes significantly between the nights, approaching its maximum in the V filter, with a difference of ≈6 mag between the two nights. To explain this discrepancy, more data and investigations are required. Of particular interest is the fact that in the first night the R an I bands present strong brightness variations with the occurrence of significant minima. The R filter also present a strong minimum during the second night, suggesting a stronger brightness dependence of the object magnitudes in the redder bands. However, before being able to impose firm constraints, other investigations are absolutely required.

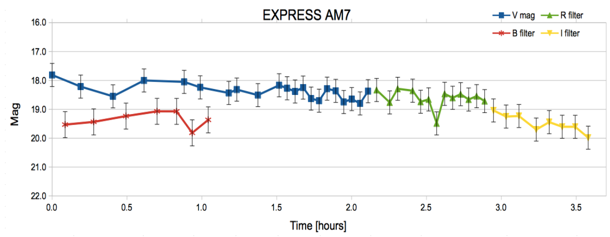

Figure 11. Multi-band lightcurves for the second night.

ACKNOWLEDGMENTS

A. D. C. would like to thank Mr. Germano Bianchi and Mr. Marco Santoro for the essential administrative support related to the internal activities for continuing the research activities. She also wants to thank Dr. Pierluigi Di Lizia and Mr. Giuseppe D'Amore for the useful suggestions they provided.

IRAF is distributed by the National Optical Astronomy Observatory, which is operated by the Association of Universities for Research in Astronomy (AURA) under a cooperative agreement with the National Science Foundation.

This work was funded by the agreement between the Italian Space Agency and the National Institute for Astrophysics "Supporto alle attivita lADC e validazione pre-operativa per SST" (ASI-INAF 2015-028-R.0).

REFERENCES

1. Bessell, M. S (1979), UBVRI photometry. II - The Cousins VRI system, its temperature and absolute flux calibration, and relevance for two-dimensional photometry, *PASP*, **91**, pp 589607
2. Cardona, T., Seitzer, P., Rossi et al. (2016). BVRI photometric observations and light-curve analysis of GEO objects, *AdSpR*, **58**, pp 514-527
3. Choi, J., Jung Hyun, J., Myung-Jin, K. et al. (2016), Determining the Rotation Periods of an Inactive LEO Satellite and the First Korean Space Debris on GEO, KOREASAT 1, *JASS*, **33**, pp 127-135
4. Cowardin, K.J., Abercromby, E.S. Barker, et al. (2009), An assessment of GEO orbital debris photometric properties derived from laboratory-based measurements. In *Proc. of AMOS Tech. Conf.*, (Ed.: S. Ryan, The Maui Economic Development Board p.E25), Maui, Hawaii
5. Jin H., Song Y., Lee Y, Kim K.S. et al. (2011), The light curves of a Geostationary Satellite and its model. In *Proc. of AMOS Tech. Conf.*, (Ed.: S. Ryan, The Maui Economic Development Board p.E64), Maui, Hawaii
6. Landolt , U. (1992), UBVRI photometric standard stars in the magnitude range 11.5-16.0 around the celestial equator, *AJ*, *vol. 104* , p. 340
7. Lederer, S. M., P. Seitzer, H. M. Cowardin et al. (2012), Characterizing Orbital Debris and Spacecrafts through a Multi-Analytical Approach. In *Proc. of AMOS Tech. Conf.*, (Ed.: S. Ryan, The Maui Economic Development Board id.77), Maui, Hawaii
8. Murtazov, A. K. (2013), Physical simulation of space objects spectral characteristics for solving the reverse problem of their photometry, *AJMP*, *Vol. 2, pp. 282-286*
9. Rossi, A., Marinoni, S., Cardona, T. et al. (2011). Physical characterization of space debris in the geosynchronous region. In 62nd International Astronautical Congress 2011, *IAC 2011* , **3**, pp. 1849-1854

10. Schildknecht, T., Musci, R., Fruh, & C. Ploner, M (2008). In *Proc. of AMOS Tech. Conf.*, (Ed.: S. Ryan, The Maui Economic Development Board p.51), Maui, Hawaii

11. Schildknecht, T., Linder, E., Silha, J. et al. (2015). Photometric Monitoring of Non-resolved Space Debris and Databases of Optical Light Curves. In *Proc. of AMOS Tech. Conf.*, (Ed.: S. Ryan, The Maui Economic Development Board id.25), Maui, Hawaii

12. Seitzer, P., Cowardin, H. M., Barker, E. et al. (2009), Photometric Studies of GEO Debris. In *Proc. of AMOS Tech. Conf.*, (Ed.: S. Ryan, The Maui Economic Development Board E23), Maui, Hawaii

13. Seo H., Jin H., Song, Y. et al. (2013), The photometric brightness variation of geostationary orbit satellite, *JASS*, **30**, pp 179–185

14. Yao, l., Chen, Z., Rongyu, S. et al. (2017), Investigations of associated multi-band observations for GEO space debris, *AdSpR*, *vol. 91*, pp 589–607